Coherence Scaling of Noisy Second-Order Scale-Free Consensus Networks

Wanyue Xu, *Graduate Student Member, IEEE*, Bin Wu, Zuobai Zhang, Zhongzhi Zhang, *Member, IEEE*, Haibin Kan, *Member, IEEE*, and Guanrong Chen, *Life Fellow, IEEE*

***Abstract*—A striking discovery in the field of network science is that the majority of real networked systems have some universal structural properties. In general, they are simultaneously sparse, scale-free, small-world, and loopy. In this article, we investigate the second-order consensus of dynamic networks with such universal structures subject to white noise at vertices. We focus on the network coherence $H_{\rm SO}$ characterized in terms of the $\mathcal{H}_2$-norm of the vertex systems, which measures the mean deviation of vertex states from their average value. We first study numerically the coherence of some representative real-world networks. We find that their coherence $H_{\rm SO}$ scales sublinearly with the vertex number N. We then study analytically $H_{\rm SO}$ for a class of iteratively growing networks—pseudofractal scale-free webs (PSFWs), and obtain an exact solution to $H_{\rm SO}$, which also increases sublinearly in N, with an exponent much smaller than 1. To explain the reasons for this sublinear behavior, we finally study $H_{\rm SO}$ for Sierpiński gaskets, for which $H_{\rm SO}$ grows superlinearly in N, with a power exponent much larger than 1. Sierpiński gaskets have the same number of vertices and edges as the PSFWs but do not display the scale-free and small-world properties. We thus conclude that the scale-free, small-world, and loopy topologies are jointly responsible for the observed sublinear scaling of $H_{\rm SO}$.**

***Index Terms*—Distributed average consensus, Gaussian white noise, multiagent systems, network coherence, scale-free network, small-world network.**

Manuscript received October 9, 2019; revised November 5, 2020; accepted January 12, 2021. This work was supported in part by the National Key Research and Development Program of China under Grant 2018YFB1305104 and Grant 2019YFB2101703; in part by the National Natural Science Foundation of China under Grant 61803248, Grant 61872093, Grant U19A2066, and Grant U20B2051; in part by the Shanghai Municipal Science and Technology Major Project under Grant 2018SHZDZX01 and ZJLab; and in part by the City University of Hong Kong under Project 7005061. This article was recommended by Associate Editor T. Huang. *(Corresponding author: Zhongzhi Zhang.)*

Wanyue Xu, Bin Wu, and Zuobai Zhang are with the Shanghai Key Laboratory of Intelligent Information Processing, School of Computer Science, Fudan University, Shanghai 200433, China (e-mail: xuwy@fudan.edu.cn; binwu11@fudan.edu.cn; 17300240035@fudan.edu.cn).

Zhongzhi Zhang and Haibin Kan are with the Shanghai Key Laboratory of Intelligent Information Processing, School of Computer Science, Fudan University, Shanghai 200433, China, and also with the Shanghai Engineering Research Institute of Blockchain, Fudan University, Shanghai 200433, China (e-mail: zhangzz@fudan.edu.cn; hbkan@fudan.edu.cn).

Guanrong Chen is with the Department of Electrical Engineering, City University of Hong Kong, Hong Kong, SAR, China (e-mail: eegchen@cityu.edu.hk).

Color versions of one or more figures in this article are available at https://doi.org/10.1109/TCYB.2021.3052519.

Digital Object Identifier 10.1109/TCYB.2021.3052519

I. Introduction

As a fundamental problem in interdisciplinary areas ranging from control systems to computer science and physics, consensus has been attracting extensive attention [1]–[6]. It can be applied to various practical scenarios, such as load balancing [7], [8]; multiagent rendezvous [9]; UAV flocking [10]; and sensor networks [11]–[13]. For multiagent systems, consensus means that the agents reach an agreement on certain quantities or values, such as load, direction, and pace. However, when the system operates in uncertain environments with noisy disturbances imposed on agents, the system will never reach consensus, with the state of each agent fluctuating around their average. In this case, what we are concerned with is the performance of the system in resisting noise.

The essence of various dynamical networks is the interaction among elements, which can be described by the powerful analytic tool—graphs, where vertices represent the elements and edges represent their relationships [14]. With this network representation, the interactions of vertex systems are organized into a complex topological structure as a network, characterized by various measurements including degree distribution, average shortest distance, and distribution of cycles or loops of different lengths. These structural properties have striking consequences on the behaviors and performance of dynamical processes running on the networked systems [15]. In the scenario of networks of agents, the consensus problem has been extensively studied, establishing nontrivial effects of network topological properties on various aspects of the problem, for example, the convergence rate [16]–[19] and robustness to time delay [19]–[21], which are determined jointly by the second smallest eigenvalue and the largest eigenvalue of the Laplacian matrix associated with the graph.

In addition to convergence rate and time delay, many other interesting quantities about consensus dynamics are also governed by the eigenvalues of the graph Laplacian matrix $\mathbf{L}$. For example, for first-order and second-order noisy networks without leaders, their network coherence defined in terms of the system's $\mathcal{H}_2$-norm (i.e., the average of deviations of agent states from the current average value) is determined by the sum of the reciprocal of the square of each nonzero eigenvalue of $\mathbf{L}$ [22]–[26]. For the first-order consensus problem, the network coherence has been studied for graphs with different structures, including the paths [27]; stars [27]; cycles [27]; Vicsek fractal trees and T-fractal trees [25], [28]; tori and lattices [24]; Farey graphs [29], [30]; Koch networks [31];

hierarchical graphs [19]; Sierpiński graphs [19]; and some real-world networks [32]. These works revealed nontrivial impacts of the network topology on the behavior of first-order network coherence.

Compared with the first-order setting, the network coherence for the second-order consensus problem is relatively rarely studied, despite the fact that it can well describe many practical applications, for example, formation control [33] and clock synchronization [34]. It has been analyzed only for several special graphs, such as tori [24]; classic fractals [19], [25], [28]; the Koch networks [31]; and hierarchical graphs [19]. However, these networks cannot well mimic most real networked systems, which exhibit universal topological properties [15]: power-law degree distribution [35], small-world behavior [36], and pattern with cycles at various scales [37], [38], where a cycle is a path plus an edge connecting its two ending nodes. It has been shown that the aggregation of these properties has a critical effect on the first-order network coherence [32]. To date, their effects on second-order network coherence are still largely unknown, which are expected to be quite different from those for the first-order case, since the intrinsic mechanisms governing their dynamics differ significantly.

To fill this gap, in this article, we study the second-order coherence of noisy consensus on networks with the aforementioned universal properties observed in many real-life networks. The main work and contribution of this article are summarized as follows.

First, we consider the coherence of scale-free small-world networks with cycles at distinct scales. We show that for these networks, the second-order coherence scales sublinearly with the number of nodes, which is in sharp contrast to their corresponding first-order coherence that converges to a constant independent of the network size [32].

Then, we address the second-order coherence of a family of deterministically iterative networks, called pseudofractal scale-free webs (PSFWs) [39]–[41], which displays some structural properties similar to those of the real networks studied. By exploiting the self-similarity of the graphs, we establish some recursion relations for the characteristic polynomials of the Laplacian matrices of the PSFWs and their subgraphs at consecutive iterations, based on which we further find exact expressions for the second-order coherence and its leading scaling, which also behaves sublinearly with the network size.

Finally, we show that the sublinear scaling for second-order coherence observed for both real and model networks lies in the composition of scale-free behavior, small-world effect, and the cycles of various scales in the considered networks. For this purpose, we study the second-order coherence of the Sierpiński gaskets [39], [40], which has the same numbers of nodes and edges as the PSFWs but are homogeneous and large world, an architecture quite different from that of PSFWs. We obtain explicit formulas for the second-order coherence and its dominating behavior, which grows superlinearly with the number of nodes.

Our results presented in this article provide insights into understanding the noisy second-order consensus dynamics and have far-reaching implications for the structural design of communication networks.

II. Preliminaries

In this section, we introduce some basic concepts about a graph, its Laplacian matrix, related distances associated with the eigenvalues and the eigenvectors of the Laplacian matrix, as well as the first-order and second-order noisy consensus problems to be studied.

A. Graph, Laplacian Matrix, and Related Distances

We use $G = (V, E)$ to denote an undirected connected graph with $N = |V|$ vertices and $M = |E|$ edges, where V is the node set, E is the edge set, and $|\cdot|$ denotes the cardinality of a set.

The adjacency matrix $\mathbf{A}$ of a graph G is an $N \times N$ symmetric matrix, representing the adjacent relations of its vertices. The entry a_{ij} of $\mathbf{A}$ at row i and column j is defined as follows: $a_{ij} = a_{ji} = 1$ if the vertex pair $(i, j) \in E$, and $a_{ij} = 0$ otherwise. Let Γ_i be the set of the neighbors for vertex i. Then, the degree of vertex i in graph G is defined as $d_i = \sum_{j=1}^{N} a_{ij} = \sum_{j\in\Gamma_i} a_{ij}$. The average degree of G is $\bar{d} = (1/N)\sum_{i=1}^{N} d_i = 2M/N$. If $\bar{d}$ is a constant, independent of N, we call G a sparse graph. For graph G, its degree matrix $\mathbf{D}$ is a diagonal matrix, with the ith diagonal entry equal to $d_i, i = 1, 2, \ldots, N$.

Let $P(d)$ be the degree distribution of graph G. If $P(d) \sim d^{-\gamma}$, we call G a scale-free network [35]. In a scale-free network, there exist some large-degree nodes, with the maximum-degree vertices called hub vertices, each having degree $d_{\max} = N^{1/(\gamma-1)}$. It has been shown [15] that many real networks are scale free.

Another important matrix related to graph G is the Laplacian matrix $\mathbf{L}$ defined by $\mathbf{L} = \mathbf{D} - \mathbf{A}$ [42]. It is an $N \times N$ positive semi-definite matrix with a unique zero eigenvalue and $N - 1$ positive eigenvalues if the graph is connected. Let λ_i, $i = 1, 2, \ldots, N$, be the N eigenvalues of $\mathbf{L}$ rearranged in ascending order, namely, $0 = \lambda_1 < \lambda_2 \leq \cdots \leq \lambda_N$. Let $\boldsymbol{u}_k$, $k = 1, 2, \ldots, N$, denote the corresponding mutually orthogonal unit eigenvectors, with the xth component being u_{kx}, $x = 1, 2, \ldots, N$. Using eigenvalues λ_k and their corresponding eigenvectors $\boldsymbol{u}_k$, $k = 1, 2, \ldots, N$, one can define various distances for a graph, such as the resistance distance and biharmonic distance. The resistance distance Ω_{ij} between two nodes i and j is [43]

$$\Omega_{ij} = \sum_{k=2}^{N} \frac{1}{\lambda_k}\left(u_{ki} - u_{kj}\right)^2 \tag{1}$$

while the biharmonic distance Θ_{ij} between i and j is defined as [44]

$$\Theta_{ij} = \sum_{k=2}^{N} \frac{1}{\lambda_k^2}\left(u_{ki} - u_{kj}\right)^2. \tag{2}$$

The sum of resistance distances over all the $N(N-1)/2$ pairs of vertices in graph G is called its Kirchhoff index [43], denoted by $R(G)$, which can be represented by all positive eigenvalues of the Laplacian matrix $\mathbf{L}$ as [45]

$$R(G) = \sum_{\substack{i,j\in V\\ i<j}} \Omega_{ij} = \frac{1}{2}\sum_{i,j\in V} \Omega_{ij} = N\sum_{i=2}^{N}\frac{1}{\lambda_i}.$$

The sum of biharmonic distances over all the $N(N-1)/2$ pairs of vertices in graph G is called its biharmonic index [26], denoted by $B(G)$. Similar to $R(G)$, $B(G)$ can be represented in terms of the $N-1$ nonzero eigenvalues of $\mathbf{L}$

$$B(G) = \sum_{\substack{i,j\in V\\ i<j}} \Theta_{ij} = N\sum_{i=2}^{N}\frac{1}{\lambda_i^2}.$$

It was shown [46] that $B(G)$ can be expressed in terms of $R(G)$ and the resistance distances of some vertex pairs.

B. Noisy First-Order Consensus Dynamics

A graph G can be considered as a multiagent system, where a vertex corresponds to an agent and an edge is associated with available information flow between two agents. In the first-order consensus network, each agent has a single state. We express the states of the system at time t by an N-dimensional real vector $x(t) \in \mathbb{R}^N$, where the ith element $x_i(t)$ represents the state of vertex i. Every agent adjusts its state according to its local information. In the presence of noise, each agent is subject to stochastic disturbances. For simplicity, we suppose that every agent is independently influenced by the Gaussian white noise with identical intensity, which is a stationary and ergodic random process with zero mean and the following fundamental property: two values of noise at any pair of times are statistically independent. Then, the evolution of the system state can be written in a matrix form as

$$\dot{x}(t) = -\mathbf{L}x(t) + w(t) \tag{3}$$

where $w(t) = (w_1(t), w_2(t), \ldots, w_N(t)) \in \mathbb{R}^N$ is a Gaussian signal with zero-mean and unit variance.

Due to the impact of noise, the agents will never reach agreement and their states fluctuate around the average value of the current states for all agents. The variance of these fluctuations can be captured by network coherence, characterized by the $\mathcal{H}_2$-norm of the system [27]. Without loss of generality, we assume that the initial condition $(1/N)\sum_{i=1}^{N} x_i(0) = 0$. The concept of network coherence represents the extent of the fluctuations [24], [25], [28],

Definition 1: For graph G, the *first-order network coherence* H_{FO} is defined as the mean steady-state variance of the deviation from the average of the current agent states

$$H_{\mathrm{FO}} := \frac{1}{N}\lim_{t\to\infty}\sum_{i=1}^{N}\mathbf{var}\left\{x_i(t) - \frac{1}{N}\sum_{j=1}^{N}x_j(t)\right\}. \tag{4}$$

It was shown [22], [24], [27], [28], [47] that H_{FO} is purely determined by the Kirchhoff index or the $N-1$ nonzero eigenvalues of $\mathbf{L}$, as given by

$$H_{\mathrm{FO}} = \frac{1}{2N}\sum_{i=2}^{N}\frac{1}{\lambda_i} = \frac{R(G)}{2N^2}. \tag{5}$$

H_{FO} measures the performance of the system robustness to noise. Low H_{FO} corresponds to good robustness, indicating that every agent keeps close to the average of the current states.

C. Noisy Second-Order Consensus Dynamics

In the second-order consensus problem, at time t, each agent i has two scalar-valued states: $x_{1,i}(t)$ and $x_{2,i}(t)$. Thus, the states of all agents can be represented by two vectors: 1) position vector $x_1(t)$ and 2) velocity vector $x_2(t)$, where $x_2(t)$ is the first-order derivative of $x_1(t)$ with respect to time t. Different from the first-order case, every agent in the second-order consensus dynamics updates its state by changing the value of $\dot{x_2}(t)$, on the basis of its own states and the states of its neighbors. The noisy second-order consensus system can be described by

$$\begin{bmatrix}\dot{x_1}(t)\\ \dot{x_2}(t)\end{bmatrix} = \begin{bmatrix}\mathbf{0} & \mathbf{I}\\ -\mathbf{L} & -\mathbf{L}\end{bmatrix}\begin{bmatrix}x_1(t)\\ x_2(t)\end{bmatrix} + \begin{bmatrix}\mathbf{0}\\ \mathbf{I}\end{bmatrix}w(t) \tag{6}$$

where vector $w(t) \in \mathbb{R}^N$ represents the uncorrelated Gaussian white noise process with zero-mean and unit variance; $\mathbf{0}$ and $\mathbf{I}$ are the $N \times N$ zero matrix and identity matrix, respectively. We note that only the variable $x_2(t)$ is subject to disturbances.

The network coherence of the above second-order dynamics only reflects the derivation of state $x_1(t)$ from the average value of the current states of all agents.

Definition 2: For graph G, the *second-order network coherence* H_{SO} is defined as the mean steady-state variance of the deviation of state $x_1(t)$ from the current average

$$H_{\mathrm{SO}} := \frac{1}{N}\lim_{t\to\infty}\sum_{i=1}^{N}\mathbf{var}\left\{x_{1,i}(t) - \frac{1}{N}\sum_{j=1}^{N}x_{1,j}(t)\right\}. \tag{7}$$

Similar to H_{FO}, H_{SO} is completely determined by the nonzero eigenvalues of the Laplacian matrix [24]. Specifically, H_{SO} is determined by the biharmonic index of the network [26]

$$H_{\mathrm{SO}} = \frac{1}{2N}\sum_{i=2}^{N}\frac{1}{\lambda_i^2} = \frac{B(G)}{2N^2}. \tag{8}$$

A low H_{SO} means that the network structure is robust to random disturbances to the second-order consensus system.

D. Related Work

The notion of network coherence was introduced by Bamieh *et al.* [24] for both noisy first-order and second-order consensus dynamics. There are many works focusing on the first-order network coherence. Young *et al.* [27] derived analytical formulas for first-order network coherence of cycles, paths, and star graphs. Patterson and Bamieh gave exact expressions for the first-order network coherence of some fractal trees [25], as well as tori and lattices [24] of different fractal dimensions. Some co-authors of the present article presented explicit solutions to the first-order network coherence in the Farey graphs [30], Koch graphs [31], self-similar hierarchical graphs [19], and Sierpiński graphs [19]. These works unveiled some nontrivial effects of network architecture on first-order network coherence. In a recent paper [32], the upper and lower bounds of the first-order network were provided for an

TABLE I
STATISTICS OF 26 REALISTIC NETWORKS. FOR A NETWORK WITH N VERTICES AND M EDGES, WE REPRESENT THE NUMBER OF VERTICES AND EDGES IN ITS LARGEST CONNECTED COMPONENT BY N' AND M', RESPECTIVELY. $\bar{d}'$ REPRESENTS THE AVERAGE DEGREE OF THE LARGEST CONNECTED COMPONENT, EQUALLING $2M'/N'$. γ DENOTES THE POWER-LAW EXPONENT. $\bar{l}$ IS THE AVERAGE SHORTEST PATH DISTANCE

Network	N	M	N'	M'	$\bar{d}'$	γ	$\bar{l}$
Karate	34	78	34	78	4.588	2.161	2.408
Windsurfers	43	336	43	336	15.628	4.001	1.671
Dolphins	62	159	62	159	5.129	5.001	3.357
Lesmis	77	254	77	254	6.597	1.521	2.641
Adjnoun	112	425	112	425	7.589	3.621	2.536
ElectronicCircuit(S208)	122	189	122	189	3.098	4.161	4.928
ElectronicCircuit(S420)	252	399	252	399	3.167	4.021	5.806
Celegansneural	297	2,148	297	2148	14.465	2.101	2.455
HamsterFull	2,426	16,631	2,000	16,098	16.098	2.421	3.588
WordAdjacency(JAP)	2,704	7,998	2,698	7,995	5.927	2.101	3.077
FacebookNIPS	4,039	88,234	4,039	88,234	43.691	2.501	3.693
GrQc	5,242	14,484	4,158	13,422	6.456	2.121	6.049
Reactome	6,327	146,160	5,973	145,778	48.812	1.741	4.214
RouteViews	6,474	12,572	6,474	12,572	3.884	2.141	3.705
WordAdjacency(SPA)	7,381	44,207	7,377	44,205	11.985	2.201	2.778
HighEnergy	7,610	15,751	5,835	13,815	4.735	3.441	7.026
HepTh	9,875	25,973	8,638	24,806	5.743	5.481	5.945
Blogcatalog	10,312	333,983	10,312	333,983	64.776	2.081	2.382
PrettyGoodPrivacy	10,680	24,316	10,680	24,316	4.554	4.261	7.486
HepPh	12,006	118,489	11,204	117,619	20.996	2.081	4.673
AstroPh	18,772	198,050	17,903	196,972	22.004	2.861	4.194
Internet	22,963	48,436	22,963	48,436	4.219	2.081	3.842
CAIDA	26,475	53,381	26,475	53,381	4.033	2.101	3.876
EnronEmail	36,692	183,831	33,696	180,811	10.732	1.981	4.025
CondensedMatter	39,577	175,692	36,458	171,735	9.421	3.681	5.499
Brightkite	58,228	214,078	56,739	212,945	7.353	2.501	4.917

arbitrary graph, where the lower bound can be approximately reached in most real-world networks.

Relative to the first-order case, related works about second-order network coherence H_{SO} are much less, with the exception of few particular graphs, such as tori [24], fractal trees [25], Koch networks [31], hierarchical graphs [19], and the Sierpiński graphs [19]. Very recently, Yi *et al.* [26] established a connection between the biharmonic distance of a graph and its second-order network coherence. They provided exact solutions to second-order network coherence of complete graphs, star graphs, cycles, and paths. However, these studied graphs cannot well mimic real-world networks, most of which are sparse, displaying simultaneously scale-free, small-world, and loopy structures. Thus far, it has not been unexplored how the second-order coherence behaves in networks with these general properties. In particular, there is no exact result about second-order coherence in scale-free, small-world, and loopy networks.

In the sequel, we study the second-order network coherence H_{SO} for scale-free, small-world, and loopy networks. First, we experimentally study various real-world networks with scale-free small-world structures and loops of different lengths. Then, we derive an exact expression for H_{SO} of a family of scale-free, small-world, and loopy networks, with the PSFWs to be detailed below. We show that their H_{SO} behaves sublinearly with the vertex number N. Finally, we obtain an explicit expression for H_{SO} of loopy Sierpiński gaskets, which are neither scale-free nor small-world but have the same number of vertices and edges as those of PSFWs. We found that the H_{SO} of the Sierpiński gaskets scales superlinearly with N. We argue that the observed sublinear scaling lies in the aggregation of scale-free, small-world, and loopy properties of the studied networks.

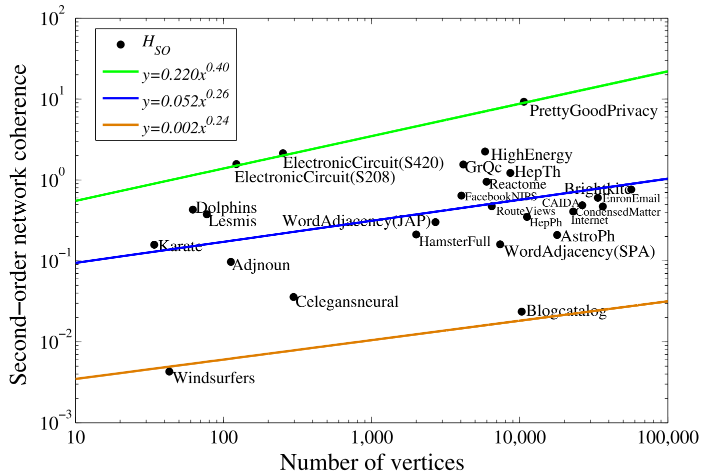

Fig. 1. Second-order network coherence H_{SO} versus vertex number in 26 realistic networks on a log–log scale. The solid lines serve as guides.

III. COHERENCE OF SOME REAL NETWORKS

In this section, we evaluate the second-order coherence for 26 real-world networks chosen from the Koblenz Network Collection [48], which are scale-free, small-world, and loopy. All these realistic networks are typical and representative, including different types of networks, such as information networks, social networks, metabolic networks, and technological networks. Table I summarizes the information of the 26 networks, listed in increasing order of their number of vertices.

Using (8), we determine the second-order coherence H_{SO} for the largest connected component of each studied network, as shown in Fig. 1. From this figure, we can observe that for all networks of different sizes, their second-order coherence H_{SO} is approximately a sublinear function of their vertex number

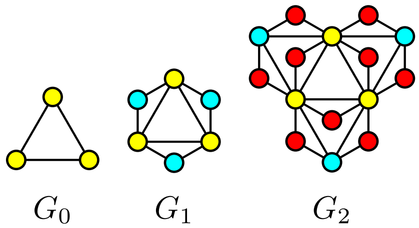

Fig. 2. First three generations of PSFWs.

N', that is, $H_{\text{SO}} \sim (N')^{\alpha}$, with $0 < \alpha < 1$. This is in sharp contrast to the first-order coherence H_{FO}, which tends to small constants much less than 1, and is independent of N' [32].

IV. Network Coherence in Pseudofractal Scale-Free Networks

In this section, we study analytically the coherence for a family of deterministic scale-free model networks, called PSFWs [39]–[41], which display some remarkable properties as observed in many real networks. It is thus expected that the behavior of the network coherence is similar to that for real networks.

A. Network Construction and Properties

The PSFWs are generated in an iterative way. We denote by G_n, the pseudofractal scale-free network after $n (n \geq 0)$ iterations. For $n = 0$, G_0 is a triangle consisting of three vertices and three edges. When $n \geq 1$, G_n is obtained from G_{n-1} as follows. Every existing edge in G_{n-1} introduces a new vertex connected to both ends of the edge. Fig. 2 illustrates the construction process for the first three generations.

Let N_n and E_n denote, respectively, the number of vertices and the number of edges in G_n. It it easy to verify that $N_n = [(3^{n+1} + 3)/2]$ and $E_n = 3^{n+1}$. In network G_n, the three vertices generated at $n = 0$ have the largest degree 2^{n+1}, which are called hub vertices and are denoted by A_n, B_n, and C_n, respectively.

The PSFWs are self-similar, which suggests another construction method highlighting their self-similar structure. This approach creating the networks is as follows. Given the nth generation network G_n, the $(n + 1)$th generation G_{n+1} is obtained by joining three copies of G_n at their hubs, see Fig. 3. Let $G_n^{(\theta)}$, $\theta = 1, 2, 3$, represent the three replicas of G_n, and let $A_n^{(\theta)}$, $B_n^{(\theta)}$, and $C_n^{(\theta)}$, $\theta = 1, 2, 3$ represent the three hub vertices of $G_n^{(\theta)}$, respectively. Then, G_{n+1} can be generated by merging $G_n^{(\theta)}$, $\theta = 1, 2, 3$, with $A_n^{(1)}$ and $B_n^{(3)}$ being identified as A_{n+1}, $B_n^{(2)}$ and $C_n^{(1)}$ being identified as B_{n+1}, and $A_n^{(2)}$ and $C_n^{(3)}$ being identified as C_{n+1}.

The PSFWs exhibit some typical properties of realistic networks. They are scale-free, with the degree distribution $P(d)$ obeying a power-law form $P(d) \sim d^{1+\ln 3/\ln 2}$ [49]. They are small-world, with the average distance scaling logarithmically with N_n. Moreover, they are highly clustered, with the average clustering coefficient converging to (4/5). Finally, they have many cycles of different lengths, the distribution of which is studied in [37].

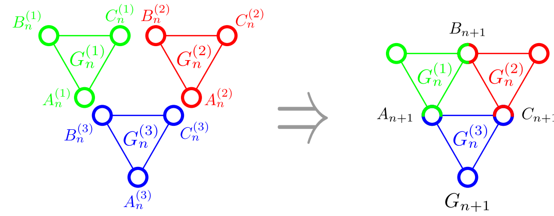

Fig. 3. Second construction of PSFWs, highlighting the self-similar property.

B. Exact Solutions and Scalings for Network Coherence

Let $\mathbf{L}_n$ denote the Laplacian matrix of network G_n, with a unique zero eigenvalue $\lambda_1(n)$ and $N_n - 1$ nonzero eigenvalues $\lambda_2(n)$, $\lambda_3(n), \ldots, \lambda_{N_n}(n)$. Let $H_{\text{FO}}(n)$ and $H_{\text{SO}}(n)$ represent, respectively, the first-order network coherence and second-order network coherence of G_n. To determine $H_{\text{FO}}(n)$ and $H_{\text{SO}}(n)$, we define two quantities S_n and T_n by $S_n = \sum_{i=2}^{N_n}(1/[\lambda_i(n)])$ and $T_n = \sum_{i=2}^{N_n}(1/[\lambda_i^2(n)])$. Then, $H_{\text{FO}}(n) = S_n/(2N_n)$ and $H_{\text{SO}}(n) = T_n/(2N_n)$. We next find S_n and T_n.

1) Recursive Relations for Related Polynomials and Quantities: To determine S_n and T_n, we introduce some quantities. Let $P_n(\lambda)$ denote the characteristic polynomial of matrix $\mathbf{L}_n$, that is

$$P_n(\lambda) = \det(\mathbf{L}_n - \lambda \mathbf{I}_n) \tag{9}$$

where $\mathbf{I}_n$ is the $N_n \times N_n$ identity matrix. Let $\mathbf{Q}_n$ be an $(N_n - 1) \times (N_n - 1)$ submatrix of $(\mathbf{L}_n - \lambda\mathbf{I}_n)$, obtained by removing from $(\mathbf{L}_n - \lambda\mathbf{I}_n)$ the row and column corresponding to a hub vertex in G_n. Let $\mathbf{R}_n$ represent a submatrix of $(\mathbf{L}_n - \lambda\mathbf{I}_n)$ with an order $(N_n - 2) \times (N_n - 2)$, obtained from $(\mathbf{L}_n - \lambda\mathbf{I}_n)$ by removing from it two rows and columns corresponding to two hub vertices in G_n. Let $\mathbf{X}_n$ represent a submatrix of $(\mathbf{L}_n - \lambda\mathbf{I}_n)$ with an order $(N_n - 1) \times (N_n - 1)$, obtained from $(\mathbf{L}_n - \lambda\mathbf{I}_n)$ by removing from it one row corresponding to a hub vertex and one column corresponding to another hub vertex. Moreover, let $Q_n(\lambda)$, $R_n(\lambda)$, $X_n(\lambda)$ denote, respectively, the determinants of $\mathbf{Q}_n$, $\mathbf{R}_n$, and $\mathbf{X}_n$. As will be shown later, S_n and T_n can be expressed in terms of the coefficients of some related polynomials.

Lemma 1: For any non-negative integer n

$$\begin{aligned} P_{n+1}(\lambda) &= 2Q_n(\lambda)^3 + 6P_n(\lambda)Q_n(\lambda)R_n(\lambda) \\ &\quad + 9\lambda Q_n(\lambda)^2 R_n(\lambda) + 3\lambda P_n(\lambda)R_n(\lambda)^2 \\ &\quad + 6\lambda^2 Q_n(\lambda)R_n(\lambda)^2 + \lambda^3 R_n(\lambda)^3 + 2X_n(\lambda)^3 \end{aligned} \tag{10}$$

$$\begin{aligned} Q_{n+1}(\lambda) &= 3Q_n(\lambda)^2 R_n(\lambda) + P_n(\lambda)R_n(\lambda)^2 \\ &\quad + 4\lambda Q_n(\lambda)R_n(\lambda)^2 + \lambda^2 R_n(\lambda)^3 \end{aligned} \tag{11}$$

$$R_{n+1}(\lambda) = 2R_n(\lambda)^2 Q_n(\lambda) + \lambda R_n(\lambda)^3 \tag{12}$$

$$\begin{aligned} X_{n+1}(\lambda) &= 2Q_n(\lambda)R_n(\lambda)X_n(\lambda) + \lambda R_n(\lambda)^2 X_n(\lambda) \\ &\quad - R_n(\lambda)X_n(\lambda)^2. \end{aligned} \tag{13}$$

Proof: By definition, P_{n+1} can be expressed as

$$P_{n+1}(\lambda) = \begin{vmatrix} 2^{n+2}-\lambda & -1 & -1 & s_n & s_n & 0 \\ -1 & 2^{n+2}-\lambda & -1 & t_n & 0 & s_n \\ -1 & -1 & 2^{n+2}-\lambda & 0 & t_n & t_n \\ s_n^{\mathrm{T}} & t_n^{\mathrm{T}} & 0 & \mathbf{R}_n & 0 & 0 \\ s_n^{\mathrm{T}} & 0 & t_n^{\mathrm{T}} & 0 & \mathbf{R}_n & 0 \\ 0 & s_n^{\mathrm{T}} & t_n^{\mathrm{T}} & 0 & 0 & \mathbf{R}_n \end{vmatrix} \tag{14}$$

where 2^{n+2} denotes the degree of the hub vertices A_{n+1}, B_{n+1}, and C_{n+1} in network G_{n+1}. s_n (t_n) is a vector of order $N_n - 2$ with $2^{n+1} - 1$ nonzero entries -1 and $N_n - 2^{n+1} - 1$ zero entries, in which each -1 describes the connection between the hub vertex A_{n+1} (B_{n+1}) and vertices belonging to $G_n^{(1)}$, $G_n^{(2)}$ or $G_n^{(3)}$, and the superscript T of a vector represents its transpose.

In a similar way, we obtain

$$Q_{n+1}(\lambda) = \begin{vmatrix} 2^{n+2}-\lambda & -1 & t_n & 0 & s_n \\ -1 & 2^{n+2}-\lambda & 0 & t_n & t_n \\ t_n^{\mathrm{T}} & 0 & \mathbf{R}_n & 0 & 0 \\ 0 & t_n^{\mathrm{T}} & 0 & \mathbf{R}_n & 0 \\ s_n^{\mathrm{T}} & t_n^{\mathrm{T}} & 0 & 0 & \mathbf{R}_n \end{vmatrix} \tag{15}$$

$$R_{n+1}(\lambda) = \begin{vmatrix} 2^{n+2}-\lambda & 0 & t_n & t_n \\ 0 & \mathbf{R}_n & 0 & 0 \\ t_n^{\mathrm{T}} & 0 & \mathbf{R}_n & 0 \\ t_n^{\mathrm{T}} & 0 & 0 & \mathbf{R}_n \end{vmatrix} \tag{16}$$

$$X_{n+1}(\lambda) = \begin{vmatrix} -1 & -1 & t_n & 0 & s_n \\ -1 & 2^{n+2}-\lambda & 0 & t_n & t_n \\ s_n^{\mathrm{T}} & 0 & \mathbf{R}_n & 0 & 0 \\ s_n^{\mathrm{T}} & t_n^{\mathrm{T}} & 0 & \mathbf{R}_n & 0 \\ 0 & t_n^{\mathrm{T}} & 0 & 0 & \mathbf{R}_n. \end{vmatrix}. \tag{17}$$

In the sequel, we will show how to derive the recursive relations for $P_{n+1}(\lambda)$, $Q_{n+1}(\lambda)$, $R_{n+1}(\lambda)$, and $X_{n+1}(\lambda)$. By the Laplace theorem, we have

$$\begin{aligned} &P_{n+1}(\lambda) \\ &= \begin{vmatrix} 2^{n+1}-\lambda & -1 & 0 & s_n & 0 & 0 \\ -1 & 2^{n+2}-\lambda & -1 & t_n & 0 & s_n \\ -1 & -1 & 2^{n+2}-\lambda & 0 & t_n & t_n \\ s_n^{\mathrm{T}} & t_n^{\mathrm{T}} & 0 & \mathbf{R}_n & 0 & 0 \\ s_n^{\mathrm{T}} & 0 & t_n^{\mathrm{T}} & 0 & \mathbf{R}_n & 0 \\ 0 & s_n^{\mathrm{T}} & t_n^{\mathrm{T}} & 0 & 0 & \mathbf{R}_n \end{vmatrix} \\ &+ \begin{vmatrix} 2^{n+1}-\lambda & 0 & -1 & 0 & s_n & 0 \\ -1 & 2^{n+2}-\lambda & -1 & t_n & 0 & s_n \\ -1 & -1 & 2^{n+2}-\lambda & 0 & t_n & t_n \\ s_n^{\mathrm{T}} & t_n^{\mathrm{T}} & 0 & \mathbf{R}_n & 0 & 0 \\ s_n^{\mathrm{T}} & 0 & t_n^{\mathrm{T}} & 0 & \mathbf{R}_n & 0 \\ 0 & s_n^{\mathrm{T}} & t_n^{\mathrm{T}} & 0 & 0 & \mathbf{R}_n \end{vmatrix} \\ &+ \lambda \begin{vmatrix} 2^{n+2}-\lambda & -1 & t_n & 0 & s_n \\ -1 & 2^{n+2}-\lambda & 0 & t_n & t_n \\ t_n^{\mathrm{T}} & 0 & \mathbf{R}_n & 0 & 0 \\ 0 & t_n^{\mathrm{T}} & 0 & \mathbf{R}_n & 0 \\ s_n^{\mathrm{T}} & t_n^{\mathrm{T}} & 0 & 0 & \mathbf{R}_n. \end{vmatrix}. \end{aligned} \tag{18}$$

According to the properties of determinants, it is straightforward to obtain (10) from (18) by using the approach in [50]. Similarly, we can derive (11)–(13). ■

2) Analytical Solutions for Intermediary Quantities: Having derived the recursive relations for the above four characteristic polynomial $P_n(\lambda)$, $Q_n(\lambda)$, $R_n(\lambda)$, and $X_n(\lambda)$, we now determine the coefficients of $P_n(\lambda)$. Define $p_n^{(i)}$ ($0 \le i \le 2$) as the coefficient of the term λ^i corresponding to $([P_n(\lambda)]/\lambda)$. Then, $p_n^{(0)}$ denotes the constant item, and $p_n^{(1)}$ and $p_n^{(2)}$ are the coefficients of the terms with degree 1 and 2, respectively.

According to Vieta's formulas, we obtain

$$S_n = \sum_{i=2}^{N_n} \frac{1}{\lambda_i(n)} = -\frac{p_n^{(1)}}{p_n^{(0)}} \tag{19}$$

$$\begin{aligned} T_n &= \sum_{i=2}^{N_n} \frac{1}{\lambda_i^2(n)} \\ &= \left(\sum_{i=2}^{N_n} \frac{1}{\lambda_i(n)}\right)^2 - 2 \sum_{2 \le i < j \le N_n} \frac{1}{\lambda_i(n)\lambda_j(n)} \\ &= S_n^2 - 2\frac{p_n^{(2)}}{p_n^{(0)}}. \end{aligned} \tag{20}$$

Thus, the problem of determining S_n and T_n is reduced to determining $p_n^{(0)}$, $p_n^{(1)}$, and $p_n^{(2)}$. In order to find these three coefficients, we introduce some additional quantities. Let $q_n^{(i)}$, $r_n^{(i)}$, and $x_n^{(i)}$, $0 \le i \le 3$, be the coefficients of term λ^i corresponding to $Q_n(\lambda)$, $R_n(\lambda)$, and $X_n(\lambda)$, respectively.

Lemma 2: For any non-negative integer n

$$p_n^{(0)} = -2^{\frac{1}{4}(-7+3^{1+n}-2n)} 3^{\frac{1}{4}(5+3^{1+n}+2n)} \left(1+3^n\right) \tag{21}$$

$$q_n^{(0)} = 2^{-\frac{3}{4}+\frac{3^{1+n}}{4}-\frac{n}{2}} 3^{\frac{1}{4}+\frac{3^{1+n}}{4}+\frac{n}{2}} \tag{22}$$

$$r_n^{(0)} = 2^{\frac{1}{4}+\frac{3^{1+n}}{4}+\frac{n}{2}} 3^{-\frac{3}{4}+\frac{3^{1+n}}{4}-\frac{n}{2}} \tag{23}$$

$$x_n^{(0)} = -2^{-\frac{3}{4}+\frac{3^{1+n}}{4}-\frac{n}{2}} 3^{\frac{1}{4}+\frac{3^{1+n}}{4}+\frac{n}{2}} \tag{24}$$

$$\begin{aligned} p_n^{(1)} &= \frac{1}{7} 2^{\frac{1}{4}(-15+3^{1+n}-2n)} 3^{\frac{1}{4}(1+3^{1+n}-2n)} \\ &\quad \times \Big(25 \times 2^n - 7 \times 3^n + 8 \times 3^{1+2n} + 25 \times 3^{1+3n} \\ &\quad + 5 \times 6^{1+n} - 35 \times 18^n\Big) \end{aligned} \tag{25}$$

$$\begin{aligned} q_n^{(1)} &= \frac{1}{7} 2^{\frac{1}{4}(-11+3^{1+n}-2n)} 3^{\frac{1}{4}(-3+3^{1+n}-2n)} \\ &\quad \times \Big(-11 \times 2^{2+n} + 7 \times 3^n - 25 \times 3^{1+2n}\Big) \end{aligned} \tag{26}$$

$$\begin{aligned} r_n^{(1)} &= \frac{1}{7} 2^{\frac{1}{4}(-7+3^{1+n}+2n)} 3^{\frac{1}{4}(-7+3^{1+n}-6n)} \\ &\quad \times \Big(3 \times 2^{2+n} - 25 \times 3^{1+2n} + 7 \times 3^n\big(-1 + 2^{2+n}\big)\Big) \end{aligned} \tag{27}$$

$$\begin{aligned} x_n^{(1)} &= \frac{1}{7} 2^{\frac{1}{4}(-11+3^{1+n}-2n)} 3^{\frac{1}{4}(-3+3^{1+n}-2n)} \\ &\quad \times \Big(2^{1+n} - 7 \times 3^n + 25 \times 3^{1+2n} - 7 \times 6^{1+n}\Big) \end{aligned} \tag{28}$$

$$\begin{aligned} p_n^{(2)} &= \frac{1}{5635} 2^{\frac{1}{4}(-27+3^{1+n}-2n)} 3^{\frac{1}{4}(-7+3^{1+n}-6n)} \\ &\quad \times \Big(-41 \times 2^{7+2n} 3^{1+n} - 9775 \times 2^{1+n} 3^{3+2n} \\ &\quad + 129283 \times 3^{1+3n} - 71875 \times 3^{3+5n} \\ &\quad + 9039 \times 4^{2+n} \\ &\quad - 20125 \times 6^{1+n} + 93541 \times 9^n \\ &\quad + 79373 \times 4^{2+n} 9^n \\ &\quad + 147163 \times 9^{1+2n} + 100625 \times 2^{1+n} 9^{1+2n} \\ &\quad - 64975 \times 54^{1+n}\Big) \end{aligned} \tag{29}$$

$$\begin{aligned} q_n^{(2)} = {} & \frac{1}{5635} 2^{\frac{1}{4}(-23+3^{1+n}-2n)} 3^{\frac{1}{4}(-11+3^{1+n}-6n)} \\ & \times \Big(8855 \times 2^{3+n}3^{1+n} - 1127 \times 2^{7+2n}3^{1+n} \\ & \quad + 71875 \times 3^{3+4n} - 18819 \times 4^{2+n} - 93541 \times 9^n \\ & \quad - 61985 \times 4^{2+n}9^n + 31625 \times 2^{3+n}9^{1+n} \\ & \quad - 36596 \times 27^{1+n}\Big) \end{aligned} \tag{30}$$

$$\begin{aligned} r_n^{(2)} = {} & \frac{1}{5635} 2^{\frac{1}{4}(-19+3^{1+n}+2n)} 3^{\frac{1}{4}(-15+3^{1+n}-10n)} \\ & \times \Big(18873 \times 2^{3+2n} + 161 \times 2^{4+2n}3^{3+n} \\ & \quad - 115 \times 2^{9+n}3^{1+2n} - 29288 \times 3^{2+3n} \\ & \quad - 20125 \times 2^{3+n}3^{2+3n} + 71875 \times 3^{3+4n} \\ & \quad - 805 \times 6^{3+n} + 127351 \times 9^n \\ & \quad - 28175 \times 2^{3+2n}9^n\Big) \end{aligned} \tag{31}$$

$$\begin{aligned} x_n^{(2)} = {} & \frac{1}{5635} 2^{\frac{1}{4}(-23+3^{1+n}-2n)} 3^{\frac{1}{4}(-11+3^{1+n}-6n)} \\ & \times \Big(1413 \times 2^{3+2n} - 805 \times 2^{2+n}3^{1+n} \\ & \quad + 1771 \times 2^{4+2n}3^{1+n} - 71875 \times 3^{3+4n} \\ & \quad + 93541 \times 9^n - 28175 \times 2^{3+2n}9^n \\ & \quad - 8165 \times 2^{4+n}9^{1+n} + 36596 \times 27^{1+n} \\ & \quad + 20125 \times 2^{2+n}27^{1+n}\Big). \end{aligned} \tag{32}$$

Proof: From (10)–(13), by using an approach similar to that in [50], it is not difficult to derive the following recursive relations governing the above-defined coefficients:

$$\begin{aligned} p_{n+1}^{(0)} = {} & 6p_n^{(0)}q_n^{(0)}r_n^{(0)} + 9\left[q_n^{(0)}\right]^2 r_n^{(0)} + 6\left[q_n^{(0)}\right]^2 q_n^{(1)} \\ & + 6\left[x_n^{(0)}\right]^2 x_n^{(1)} \end{aligned} \tag{33}$$

$$q_{n+1}^{(0)} = 3\left[q_n^{(0)}\right]^2 r_n^{(0)} \tag{34}$$

$$r_{n+1}^{(0)} = 2q_n^{(0)}\left[r_n^{(0)}\right]^2 \tag{35}$$

$$x_{n+1}^{(0)} = 2q_n^{(0)}r_n^{(0)}x_n^{(0)} - r_n^{(0)}\left[x_n^{(0)}\right]^2 \tag{36}$$

$$\begin{aligned} p_{n+1}^{(1)} = {} & 3p_n^{(0)}\left[r_n^{(0)}\right]^2 + 6q_n^{(0)}\left[r_n^{(0)}\right]^2 + 6q_n^{(0)}r_n^{(0)}p_n^{(1)} \\ & + 6p_n^{(0)}r_n^{(0)}q_n^{(1)} + 18q_n^{(0)}r_n^{(0)}q_n^{(1)} + 6q_n^{(0)}\left[q_n^{(1)}\right]^2 \\ & + 6p_n^{(0)}q_n^{(0)}r_n^{(1)} + 9\left[q_n^{(0)}\right]^2 r_n^{(1)} + 6x_n^{(0)}\left[x_n^{(1)}\right]^2 \\ & + \left[6q_n^{(0)}\right]^2 q_n^{(2)} + 6\left[x_n^{(0)}\right]^2 x_n^{(2)} \end{aligned} \tag{37}$$

$$\begin{aligned} q_{n+1}^{(1)} = {} & p_n^{(0)}\left[r_n^{(0)}\right]^2 + 4q_n^{(0)}\left[r_n^{(0)}\right]^2 + 6q_n^{(0)}r_n^{(0)}q_n^{(1)} \\ & + 3\left[q_n^{(0)}\right]^2 r_n^{(1)} \end{aligned} \tag{38}$$

$$r_{n+1}^{(1)} = \left[r_n^{(0)}\right]^3 + 2\left[r_n^{(0)}\right]^2 q_n^{(1)} + 4q_n^{(0)}r_n^{(0)}r_n^{(1)} \tag{39}$$

$$\begin{aligned} x_{n+1}^{(1)} = {} & \left[r_n^{(0)}\right]^2 x_n^{(0)} + 2r_n^{(0)}x_n^{(0)}q_n^{(1)} + 2q_n^{(0)}x_n^{(0)}r_n^{(1)} \\ & - \left[x_n^{(0)}\right]^2 r_n^{(1)} + 2q_n^{(0)}r_n^{(0)}x_n^{(1)} - 2r_n^{(0)}x_n^{(0)}x_n^{(1)} \end{aligned} \tag{40}$$

$$\begin{aligned} p_{n+1}^{(2)} = {} & \left[r_n^{(0)}\right]^3 + 3\left[r_n^{(0)}\right]^2 p_n^{(1)} + 6\left[r_n^{(0)}\right]^2 q_n^{(1)} + 6r_n^{(0)}p_n^{(1)} \\ & q_n^{(1)} + 9r_n^{(0)}\left[q_n^{(1)}\right]^2 + 2\left[q_n^{(1)}\right]^3 + 6p_n^{(0)}r_n^{(0)}r_n^{(1)} \\ & + 12q_n^{(0)}r_n^{(0)}r_n^{(1)} + 6q_n^{(0)}p_n^{(1)}r_n^{(1)} + 6p_n^{(0)}q_n^{(1)}r_n^{(1)} \\ & + 18q_n^{(0)}q_n^{(1)}r_n^{(1)} + 2\left[x_n^{(1)}\right]^3 + 6q_n^{(0)}r_n^{(0)}p_n^{(2)} \\ & + 6p_n^{(0)}r_n^{(0)}q_n^{(2)} + 18q_n^{(0)}r_n^{(0)}q_n^{(2)} + 12q_n^{(0)}q_n^{(1)}q_n^{(2)} \\ & + 6p_n^{(0)}q_n^{(0)}r_n^{(2)} + 9\left[q_n^{(0)}\right]^2 r_n^{(2)} + 12x_n^{(0)}x_n^{(1)}x_n^{(2)} \\ & + 6\left[q_n^{(0)}\right]^2 q_n^{(3)} + 6\left[x_n^{(0)}\right]^2 x_n^{(3)} \end{aligned} \tag{41}$$

$$\begin{aligned} q_{n+1}^{(2)} = {} & \left[r_n^{(0)}\right]^3 + \left[r_n^{(0)}\right]^2 p_n^{(1)} + 4\left[r_n^{(0)}\right]^2 q_n^{(1)} + 3r_n^{(0)} \\ & \left[q_n^{(1)}\right]^2 + 2p_n^{(0)}r_n^{(0)}r_n^{(1)} + 8q_n^{(0)}r_n^{(0)}r_n^{(1)} + 6q_n^{(0)} \\ & q_n^{(1)}r_n^{(1)} + 6q_n^{(0)}r_n^{(0)}q_n^{(2)} + 3\left[q_n^{(0)}\right]^2 r_n^{(2)} \end{aligned} \tag{42}$$

$$\begin{aligned} r_{n+1}^{(2)} = {} & 3\left[r_n^{(0)}\right]^2 r_n^{(1)} + 4r_n^{(0)}q_n^{(1)}r_n(1) + 2q_n^{(0)}\left[r_n^{(1)}\right]^2 \\ & + 2\left[r_n^{(0)}\right]^2 q_n^{(2)} + 4q_n^{(0)}r_n^{(0)}r_n^{(2)} \end{aligned} \tag{43}$$

$$\begin{aligned} x_{n+1}^{(2)} = {} & 2r_n^{(0)}x_n^{(0)}r_n^{(1)} + 2x_n^{(0)}q_n^{(1)}r_n^{(1)} + \left[r_n^{(0)}\right]^2 x_n^{(1)} \\ & + 2r_n^{(0)}q_n^{(1)}x_n^{(1)} + 2q_n^{(0)}r_n^{(1)}x_n^{(1)} - 2x_n^{(0)}r_n^{(1)}x_n^{(1)} \\ & - r_n^{(0)}\left[x_n^{(1)}\right]^2 + 2r_n^{(0)}x_n^{(0)}q_n^{(2)} + 2q_n^{(0)}x_n^{(0)}r_n^{(2)} \\ & - \left[x_n^{(0)}\right]^2 r_n^{(2)} + 2q_n^{(0)}r_n^{(0)}x_n^{(2)} - 2r_n^{(0)}x_n^{(0)}x_n^{(2)} \end{aligned} \tag{44}$$

$$\begin{aligned} q_{n+1}^{(3)} = {} & 3\left[r_n^{(0)}\right]^2 r_n^{(1)} + 2r_n^{(0)}p_n^{(1)}r_n^{(1)} + 8r_n^{(0)}q_n^{(1)}r_n^{(1)} \\ & + 3\left[q_n^{(1)}\right]^2 r_n^{(1)} + p_n^{(0)}\left[r_n^{(1)}\right]^2 + 4q_n^{(0)}\left[r_n^{(1)}\right]^2 \\ & + \left[r_n^{(0)}\right]^2 p_n^{(2)} + 4\left[r_n^{(0)}\right]^2 q_n^{(2)} + 6r_n^{(0)}q_n^{(1)}q_n^{(2)} \\ & + 6q_n^{(0)}r_n^{(1)}q_n^{(2)} + 2p_n^{(0)}r_n^{(0)}r_n^{(2)} + 8q_n^{(0)}r_n^{(0)}r_n^{(2)} \\ & + 6q_n^{(0)}q_n^{(1)}r_n^{(2)} + 6q_n^{(0)}r_n^{(0)}q_n^{(3)} + 3\left[q_n^{(0)}\right]^2 r_n^{(3)} \end{aligned} \tag{45}$$

$$\begin{aligned} r_{n+1}^{(3)} = {} & 3r_n^{(0)}\left[r_n^{(1)}\right]^2 + 2q_n^{(1)}\left[r_n^{(1)}\right]^2 + 4r_n^{(0)}r_n^{(1)}q_n^{(2)} \\ & + 3\left[r_n^{(0)}\right]^2 r_n^{(2)} + 4r_n^{(0)}q_n^{(1)}r_n^{(2)} + 4q_n^{(0)}r_n^{(1)}r_n^{(2)} \\ & + 2\left[r_n^{(0)}\right]^2 q_n^{(3)} + 4q_n^{(0)}r_n^{(0)}r_n^{(3)} \end{aligned} \tag{46}$$

$$\begin{aligned} x_{n+1}^{(3)} = {} & x_n^{(0)}\left[r_n^{(1)}\right]^2 + 2r_n^{(0)}r_n^{(1)}x_n^{(1)} + 2q_n^{(1)}r_n^{(1)}x_n^{(1)} \\ & - r_n^{(1)}\left[x_n^{(1)}\right]^2 + 2x_n^{(0)}r_n^{(1)}q_n^{(2)} + 2r_n^{(0)}x_n^{(1)}q_n^{(2)} \\ & + 2r_n^{(0)}x_n^{(0)}r_n^{(2)} + 2x_n^{(0)}q_n^{(1)}r_n^{(2)} + 2q_n^{(0)}x_n^{(1)}r_n^{(2)} \\ & - 2x_n^{(0)}x_n^{(1)}r_n^{(2)} + \left[r_n^{(0)}\right]^2 x_n^{(2)} + 2r_n^{(0)}q_n^{(1)}x_n^{(2)} \\ & + 2q_n^{(0)}r_n^{(1)}x_n^{(2)} - 2x_n^{(0)}r_n^{(1)}x_n^{(2)} - 2r_n^{(0)}x_n^{(1)}x_n^{(2)} \\ & + 2r_n^{(0)}x_n^{(0)}q_n^{(3)} + 2q_n^{(0)}x_n^{(0)}r_n^{(3)} - \left[x_n^{(0)}\right]^2 r_n^{(3)} \\ & + 2q_n^{(0)}r_n^{(0)}x_n^{(3)} - 2r_n^{(0)}x_n^{(0)}x_n^{(3)}. \end{aligned} \tag{47}$$

With the initial values $p_0^{(0)} = -9$, $q_0^{(0)} = 3$, $r_0^{(0)} = 2$, $x_0^{(0)} = 3$, $p_0^{(1)} = 6$, $q_0^{(1)} = -4$, $r_0^{(1)} = -1$, $x_0^{(1)} = 1$, $p_0^{(2)} = -1$, $q_0^{(2)} = -1$, $r_0^{(2)} = 0$, and $x_0^{(2)} = 0$, (33)–(47) can be solved to obtain (21)–(32). Due to the space limitation, below we only derive $q_n^{(0)}$, $r_n^{(0)}$, and $x_n^{(0)}$, the other quantities can be obtained in a similar way.

Equation (35) can be rewritten as

$$q_n^{(0)} = \frac{r_{n+1}^{(0)}}{2\left[r_n^{(0)}\right]^2}. \tag{48}$$

Inserting (48) into (34) leads to

$$\frac{r_{n+2}^{(0)}}{\left[r_{n+1}^{(0)}\right]^3} = \frac{3r_{n+1}^{(0)}}{2\left[r_n^{(0)}\right]^3} \tag{49}$$

which provides an explicit recursive relation governing $r_n^{(0)}$, $r_{n+1}^{(0)}$, and $r_{n+2}^{(0)}$.

We now derive a closed-form expression for $r_n^{(0)}$. To this end, we introduce an intermediary quantity k_n, defined as

$$k_n = \frac{r_n^{(0)}}{\left[r_{n-1}^{(0)}\right]^3} \tag{50}$$

which, together with (49), yields

$$k_{n+1} = \frac{3}{2}k_n. \tag{51}$$

Using the initial condition $k_1 = r_1^{(0)}/[r_0^{(0)}]^3 = 3$, (51) is solved to give

$$k_n = 2\left(\frac{3}{2}\right)^n. \tag{52}$$

With this exact result of k_n, (50) is recast as

$$\ln r_n^{(0)} = 3 \ln r_{n-1}^{(0)} + \ln k_n^{(0)}. \tag{53}$$

Considering $\ln r_0^{(0)} = \ln 2$ and the expression for k_n given in (52), (53) is solved inductively to yield

$$\ln r_n^{(0)} = 3^n \ln r_0^{(0)} + \sum_{i=0}^{n-1} 3^i \ln \left[2\left(\frac{3}{2}\right)^{i+1}\right] \tag{54}$$

which implies

$$r_n^{(0)} = 2^{\frac{1}{4}+\frac{3^{1+n}}{4}+\frac{n}{2}}3^{-\frac{3}{4}+\frac{3^{1+n}}{4}-\frac{n}{2}}$$

as shown in (23).

After deriving $r_n^{(0)}$, we continue to calculate $q_n^{(0)}$. Plugging (23) into (48) gives

$$q_n^{(0)} = 2^{-\frac{3}{4}+\frac{3^{1+n}}{4}-\frac{n}{2}}3^{\frac{1}{4}+\frac{3^{1+n}}{4}+\frac{n}{2}}.$$

In this way, we obtain (22). Finally, we determine $x_n^{(0)}$. By inserting (34) into (36), one obtains

$$\frac{x_{n+1}^{(0)}}{q_{n+1}^{(0)}} = \frac{2x_n^{(0)}}{3q_n^{(0)}} - \frac{1}{3}\left[\frac{x_n^{(0)}}{q_n^{(0)}}\right]^2. \tag{55}$$

In order to obtain the exact expression for $x_n^{(0)}$, we introduce another quantity y_n defined by

$$y_n = \frac{x_n^{(0)}}{q_n^{(0)}}. \tag{56}$$

Then, (55) can be rewritten as

$$y_{n+1} = \frac{2}{3}y_n - \frac{1}{3}y_n^2 \tag{57}$$

which, under the initial condition $y_0 = x_0^{(0)}/q_0^{(0)} = -1$, is solved to yield

$$y_n = -1. \tag{58}$$

Combine (58), (56), and $r_n^{(0)}$, we obtain

$$x_n^{(0)} = -2^{-\frac{3}{4}+\frac{3^{1+n}}{4}-\frac{n}{2}}3^{\frac{1}{4}+\frac{3^{1+n}}{4}+\frac{n}{2}}$$

as provided by (24). ■

3) Explicit Expression and Behavior for Network Coherence: With the above-obtained quantities, we can obtain accurate solutions for both the first-order and the second-order network coherence of network G_n, from which we can further reveal their asymptotical behaviors.

Theorem 1: For the PSFW G_n with $n \geq 1$, the first-order coherence $H_{\rm FO}(n)$ and second-order coherence $H_{\rm SO}(n)$ of the system with dynamics in (5) and (8) are

$$\begin{aligned} H_{\rm FO}(n) = \frac{1}{28(1+3^n)^2 3^{2+n}} \times \big(&25 \times 2^n \\ &- 7 \times 3^n + 8 \times 3^{1+2n} + 25 \times 3^{1+3n} \\ &+ 5 \times 6^{1+n} - 35 \times 18^n\big) \end{aligned} \tag{59}$$

$$\begin{aligned} H_{\rm SO}(n) = \frac{3^{-4-2n}}{90160(1+3^n)^3} \times \Big(&69538 \times 3^{2+5n} + 360249 \\ &\times 4^n + 35 \times 2^{2+n}3^{1+n}\big(-575 + 1539 \times 2^n\big) \\ &+ 322 \times 27^n\Big(1135 - 3225 \times 2^{1+n} + 847 \times 2^{1+2n}\Big) \\ &+ 3^{1+4n}\Big(516262 - 60375 \times 2^{2+n} + 140875 \times 4^n\Big) \\ &+ 2 \times 9^n\Big(55223 - 94875 \times 2^{1+n} + 480487 \times 4^n\Big)\Big). \end{aligned} \tag{60}$$

Moreover

$$\lim_{n\to\infty} H_{\rm FO}(n) = \frac{25}{84} \tag{61}$$

$$\lim_{n\to\infty} H_{\rm SO}(n) = \frac{25}{432}(N_n)^{(\log_3 4)-1}. \tag{62}$$

Proof: Since $H_{\rm FO}(n) = S_n/(2N_n)$ and $H_{\rm SO}(n) = T_n/(2N_n)$, combining the above-obtained related quantities and using (19) and (20), we obtain (59) and (60), which lead to (61) and (62) for sufficiently large n. ■

Notice that (59) and (61) were previously obtained in [32] by using a different technique. However, (60) and (62) are novel. Theorem 1 shows that in large networks G_n, the first-order coherence $H_{\rm FO}(n)$ does not depend on n, thus not on N_n, while the second-order coherence $H_{\rm SO}(n)$ increases sublinearly with N_n.

V. Network Coherence in Sierpiński Gaskets

In the previous section, we obtained an explicit formula of network coherence $H_{\rm FO}(n)$ for PSFW G_n, and showed that $H_{\rm FO}(n)$ is a sublinear function of N_n. To unveil the effect of scale-free and small-world topologies on the scaling of

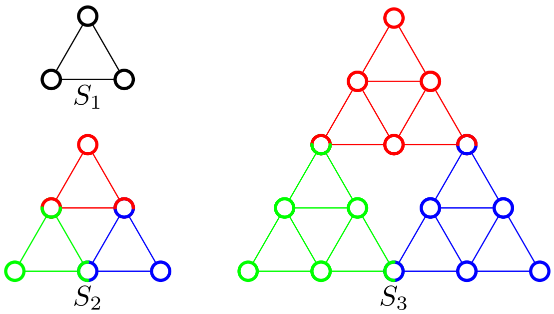

Fig. 4. First three generations of the Sierpiński gaskets.

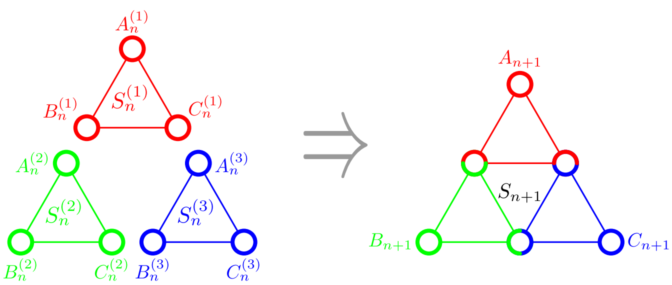

Fig. 5. Second construction of the Sierpiński gaskets, highlighting the self-similar structure.

network coherence, in this section we derive an analytical expression for network coherence in the Sierpiński gaskets with the same numbers of vertices and edges as those of PSFWs. We will show that the leading scalings of both first-order and second-order network coherence for S_n are significantly different from those associated with G_n.

The Sierpiński gaskets are also iteratively constructed. Let S_n ($n \geq 0$) denote the networks after n iterations. Then, the Sierpiński gaskets are generated as follows. When $n = 0$, S_0 is an equilateral triangle with three vertices and three edges. For $n = 1$, the three edges of the equilateral triangle S_0 are bisected and the central triangle is removed, yielding S_1 containing three copies of the original triangle. For $n \geq 1$, S_n is generated from S_{n-1} by performing the bisection and removal procedure for each upward-pointing triangle in S_{n-1}. Fig. 4 illustrates the first three generations of Sierpiński gaskets.

Both the number of vertices and the number of edges in S_n are the same as those of G_n. That is, there are $N_n = [(3^{n+1} + 3)/2]$ vertices and $E_n = 3^{n+1}$ edges in S_n. Many other properties of S_n and G_n are quite different from each other. For example, Sierpiński gaskets are neither scale-free nor small-world. They are homogeneous, with the degrees of the three outmost vertices equal to 2, while the degrees of other vertices being 4.

Despite the difference between S_n and G_n, there are some similarity between them. For instance, both graphs have cycles of various lengths. Moreover, Sierpiński gaskets are likewise self-similar, as can be seen from the following alternative construction approach. We denote the three outmost vertices in S_n with degree 2 by A_n, B_n, and C_n, respectively. Then, S_{n+1} is obtained from S_n by joining three copies of S_n at their outmost vertices, as shown in Fig. 5. Let $S_n^{(\theta)}$, $\theta = 1, 2, 3$, represent the three replicas of S_n, with outmost vertices $A_n^{(\theta)}$, $B_n^{(\theta)}$, and $C_n^{(\theta)}$. Then, S_{n+1} is created by coalescing $S_n^{(\theta)}$, $\theta = 1, 2, 3$, with $A_n^{(1)}$, $B_n^{(2)}$, and $C_n^{(3)}$ being the three outmost vertices of S_{n+1}.

Let $H_{\mathrm{FO}}(n)$ and $H_{\mathrm{SO}}(n)$ denote, respectively, the first-order network coherence and second-order network coherence for S_n. By using a similar method and procedure, we can obtain exact solutions for $H_{\mathrm{FO}}(n)$ and $H_{\mathrm{SO}}(n)$ and the leading scalings for S_n, as summarized in the following theorem.

Theorem 2: For the Sierpiński gasket S_n with $n \geq 1$, the first-order coherence $H_{\mathrm{FO}}(n)$ and the second-order coherence $H_{\mathrm{SO}}(n)$ of the system with dynamics in (5) and (8) are

$$\begin{aligned} H_{\mathrm{FO}}(n) = {} & \frac{1}{20 \times 3^{2+n}(1+3^n)^2} \\ & \times \Big(4 \times 3^n + 2 \times 3^{1+2n} - 3^{1+3n} + 13 \times 3^{1+n}5^n \\ & \quad + 4 \times 5^{1+n} + 14 \times 45^n\Big) \end{aligned} \tag{63}$$

$$\begin{aligned} H_{\mathrm{SO}}(n) = {} & \frac{1}{400(1+3^n)^3 9^{2+n}} \\ & \times \Big(86 \times 3^{1+4n} - 2 \times 3^{2+5n} + 754 \times 3^{1+2n}5^n \\ & + 568 \times 3^{1+3n}5^n + 32 \times 3^{2+n}5^{1+2n} + 119 \times 9^n \\ & + 28 \times 5^n 9^{1+2n} + 64 \times 15^{1+n} + 8 \\ & \times 9^{1+2n}25^n + 24 \times 25^{1+n} + 320 \times 27^n \\ & + 1237 \times 225^n + 394 \times 675^n\Big). \end{aligned} \tag{64}$$

Moreover

$$\lim_{n\to\infty} H_{\mathrm{FO}}(n) = \frac{7}{90}(N_n)^{(\log_3 5)-1} \tag{65}$$

and

$$\lim_{n\to\infty} H_{\mathrm{SO}}(n) = \frac{1}{450}(N_n)^{(\log_3 25)-1}. \tag{66}$$

Theorem 2 shows that the behaviors of both first-order coherence $H_{\mathrm{FO}}(n)$ and second-order coherence $H_{\mathrm{SO}}(n)$ in the Sierpiński gaskets significantly differ from those of PSFWs. For large Sierpiński gaskets S_n, the first-order coherence $H_{\mathrm{FO}}(n)$ increases sublinearly with N_n, while the second-order coherence $H_{\mathrm{SO}}(n)$ behaves superlinearly with N_n.

In Fig. 6, we report a direct comparison of approximate and exact results about first-order coherence $H_{\mathrm{FO}}(n)$ and second-order coherence $H_{\mathrm{SO}}(n)$ in PSFWs G_n and the Sierpiński gaskets S_n for various n. For moderately large n, the exact and approximate results agree with each other.

VI. Result Analysis

In the previous sections, we have investigated the noisy second-order consensus dynamics of some real-life scale-free networks and a class of scale-free model networks. For all these studied scale-free networks, their second-order network coherence scales sublinearly with the number of vertices N. Note that for a network, its second-order coherence is completely determined by the sum of the square reciprocal of every nonzero eigenvalue of its Laplacian matrix. Since for scale-free networks, the eigenvalues and their distributions are closely related to the network structures [51], the sublinear scaling for coherence observed for the considered scale-free networks lies in their intrinsic structural characteristics, in particular, the scale-free small-world topology and cycles of different lengths.

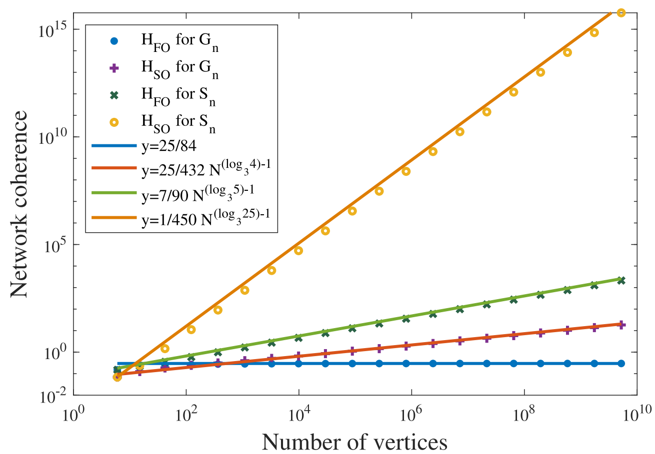

Fig. 6. First-order and second-order network coherences versus N_n in both G_n and S_n on a log-log scale, with n changing from 1 to 20. The exact results of G_n are calculated by (59) and (60), while the explicit results of S_n are obtained by (63) and (64). The approximate results are obtained by (61) and (62) for G_n, and by (65) and (66) for S_n.

As shown in [26], the second-order coherence of a network is determined by the average of biharmonic distances Θ_{ij} over all pairs of vertices. By formulas (1) and (2), for any pair of vertices i and j, both resistance distance Ω_{ij} and biharmonic distance Θ_{ij} are combinations of $(1/\lambda_k)(u_{ki} - u_{kj})^2$, $k = 1, 2, \ldots, N-1$. For the resistance distance, the weight of each term is 1, while for the biharmonic distance, the weight varies, with a larger term $(1/\lambda_k)(u_{ki} - u_{kj})^2$ corresponding to a larger weight $(1/\lambda_k)$. Thus, for most graphs, Θ_{ij} is greater than Ω_{ij}. In a scale-free network, the existence of large-degree vertices connected to many other vertices is accompanied by the small-world property, characterized by at most a logarithmical growth average path length [15]. Moreover, for a scale-free small-world network, its average resistance distance is even smaller, converging to a constant [32]. In contrast to the constant average resistance distance, the average of biharmonic distances is dependent on N, scaling sublinearly with N. Next, we show that this sublinear scaling is an aggregation of scale-free, small-world, and loopy structures, since neither power-law small-world behavior nor cycles alone can ensure a sublinear coherence, but it leads to linear or superlinear scaling.

It was reported that for the scale-free small-world Koch network [31], its second-order network coherence H_{SO} behaves linearly with the number of vertices N, which is also observed for the small-world hierarchical graphs [19] with an exponential degree distribution. Both Koch networks and hierarchical graphs are highly clustered but have only small cycles such as triangles, lacking cycles of various lengths. Thus, the existence of cycles of different lengths is necessary for sublinear scaling of H_{SO} in a network. However, cycles do not suffice to guarantee a sublinear scaling of H_{SO}. For example, in the Sierpiński gaskets, there are cycles of various lengths, but their H_{SO} is a superlinear function of N as given by formula (66). This, in turn, indicates that scale-free small-world topology is only necessary for a sublinear scaling of H_{SO} in a sparse network.

Note that although the small-world is an accompanying phenomenon of the power-law behavior [15], small-world and loopy structures cannot lead to the sublinear scaling of second-order network coherence. For example, using the result in [30] and the technique in this current article, we can determine the analytical expression of second-order coherence for the Farey graphs, which scales linearly with the number of nodes, being quite different from the sublinear scaling observed for the PSFWs. By construction, the Farey graphs are subgraphs of PSFWs, both of which are small world and highly clustered, with many cycles at different scales. The reason for the scaling distinction of the second-order coherence between the Farey graphs and PSFWs lies in, at least partially, the scale-free topology of PSFWs that the Farey graphs do not possess.

VII. Conclusion

A large variety of real-world networks are sparse and loopy and exhibit simultaneously scale-free and small-world features. These structural properties have a substantial influence on different dynamics running on such networks. In this article, we presented an extensive study on second-order consensus in noisy networks with these properties, focusing on its robustness measured by network coherence that is characterized by the average steady-state variance of the system. We first studied numerically the network coherence for some representative real scale-free networks, which grows sublinearly with the vertex number N. We then determined exactly the coherence for a class of deterministic scale-free networks, PSFWs, which is also a sublinear function of N. Moreover, we studied analytically the coherence for Sierpiński gaskets with the same numbers of vertices and edges as the PSFWs, the leading scaling of which scales superlinearly in N. We concluded that the scale-free, small-world, and loopy structures are responsible for the observed sublinear scaling of coherence for the studied networks.

It should be mentioned that we only addressed second-order noisy consensus on undirected binary networks, concentrating on scale-free, small-world, and loopy properties on the effects of network coherence. Future work should include the following directions. First, it would be of interest to consider second-order noisy consensus on directed [52], [53] and weighted [54], [55] communication graphs, with an aim to explore the influences of one-way action or distribution of edge weights on network coherence. Another direction is to examine second-order noisy linear consensus networks in the presence of time delay [56], [57]. Moreover, of particular interest is to consider the case that both scalar-valued states of each agent are subject to disturbances. Finally, our method and process for computing the network coherence are only applicable to deterministically growing self-similar networks, it is of great significance to modify or extend them to more general networks.

References

[1] M. Barborak, A. Dahbura, and M. Malek, “The consensus problem in fault-tolerant computing,” *ACM Comput. Surveys*, vol. 25, no. 2, pp. 171–220, 1993.

[2] R. Olfati-Saber, J. A. Fax, and R. M. Murray, "Consensus and cooperation in networked multi-agent systems," *Proc. IEEE*, vol. 95, no. 1, pp. 215–233, Jan. 2007.

[3] Y. Cao, W. Yu, W. Ren, and G. Chen, "An overview of recent progress in the study of distributed multi-agent coordination," *IEEE Trans. Ind. Informat.*, vol. 9, no. 1, pp. 427–438, Feb. 2013.

[4] S. Motsch and E. Tadmor, "Heterophilious dynamics enhances consensus," *SIAM Rev.*, vol. 56, no. 4, pp. 577–621, 2014.

[5] X. Wu, Y. Tang, J. Cao, and W. Zhang, "Distributed consensus of stochastic delayed multi-agent systems under asynchronous switching," *IEEE Trans. Cybern.*, vol. 46, no. 8, pp. 1817–1827, Aug. 2016.

[6] X. Shi, J. Cao, and W. Huang, "Distributed parametric consensus optimization with an application to model predictive consensus problem," *IEEE Trans. Cybern.*, vol. 48, no. 7, pp. 2024–2035, Jul. 2017.

[7] R. Diekmann, A. Frommer, and B. Monien, "Efficient schemes for nearest neighbor load balancing," *Parallel Comput.*, vol. 25, no. 7, pp. 789–812, 1999.

[8] N. Amelina, A. Fradkov, Y. Jiang, and D. J. Vergados, "Approximate consensus in stochastic networks with application to load balancing," *IEEE Trans. Inf. Theory*, vol. 61, no. 4, pp. 1739–1752, Apr. 2015.

[9] D. V. Dimarogonas and K. J. Kyriakopoulos, "On the rendezvous problem for multiple nonholonomic agents," *IEEE Trans. Autom. Control*, vol. 52, no. 5, pp. 916–922, May 2007.

[10] R. Olfati-Saber, "Flocking for multi-agent dynamic systems: Algorithms and theory," *IEEE Trans. Autom. Control*, vol. 51, no. 3, pp. 401–420, Mar. 2006.

[11] Q. Li and D. Rus, "Global clock synchronization in sensor networks," *IEEE Trans. Comput.*, vol. 55, no. 2, pp. 214–226, Feb. 2006.

[12] W. Yu, G. Chen, Z. Wang, and W. Yang, "Distributed consensus filtering in sensor networks," *IEEE Trans. Syst., Man, Cybern. B, Cybern.*, vol. 39, no. 6, pp. 1568–1577, Dec. 2009.

[13] S. Zhu, C. Chen, W. Li, B. Yang, and X. Guan, "Distributed optimal consensus filter for target tracking in heterogeneous sensor networks," *IEEE Trans. Cybern.*, vol. 43, no. 6, pp. 1963–1976, Dec. 2013.

[14] M. E. J. Newman, *Networks: An Introduction*. Oxford, U.K.: Oxford Univ. Press, 2010.

[15] M. E. J. Newman, "The structure and function of complex networks," *SIAM Rev.*, vol. 45, no. 2, pp. 167–256, Jun. 2003.

[16] R. Olfati-Saber, "Ultrafast consensus in small-world networks," in *Proc. Amer. Control Conf.*, 2005, pp. 2371–2378.

[17] A. Olshevsky and J. N. Tsitsiklis, "Convergence speed in distributed consensus and averaging," *SIAM J. Control Optim.*, vol. 48, no. 1, pp. 33–55, 2009.

[18] T. C. Aysal and K. E. Barner, "Convergence of consensus models with stochastic disturbances," *IEEE Trans. Inf. Theory*, vol. 56, no. 8, pp. 4101–4113, Aug. 2010.

[19] Y. Qi, Z. Zhang, Y. Yi, and H. Li, "Consensus in self-similar hierarchical graphs and Sierpinski graphs: Convergence speed, delay robustness, and coherence," *IEEE Trans. Cybern.*, vol. 49, no. 2, pp. 592–603, Feb. 2019.

[20] F. Xiao and L. Wang, "Consensus protocols for discrete-time multi-agent systems with time-varying delays," *Automatica*, vol. 44, no. 10, pp. 2577–2582, 2008.

[21] U. Münz, A. Papachristodoulou, and F. Allgäwer, "Delay robustness in consensus problems," *Automatica*, vol. 46, no. 8, pp. 1252–1265, 2010.

[22] L. Xiao, S. Boyd, and S.-J. Kim, "Distributed average consensus with least-mean-square deviation," *J. Parallel. Distrib. Comput.*, vol. 67, no. 1, pp. 33–46, Jan. 2007.

[23] S. Patterson and B. Bamieh, "Leader selection for optimal network coherence," in *Proc. 49th IEEE Conf. Decis. Control*, 2010, pp. 2692–2697.

[24] B. Bamieh, M. Jovanovic R. P. Mitra, and S. Patterson, "Coherence in large-scale networks: Dimension-dependent limitations of local feedback," *IEEE Trans. Autom. Control*, vol. 57, no. 9, pp. 2235–2249, Sep. 2012.

[25] S. Patterson and B. Bamieh, "Consensus and coherence in fractal networks," *IEEE Trans. Control Netw. Syst.*, vol. 1, no. 4, pp. 338–348, Sep. 2014.

[26] Y. Yi, B. Yang, Z. Zhang, and S. Patterson, "Biharmonic distance and the performance of second-order consensus networks with stochastic disturbances," in *Proc. Amer. Control Conf.*, 2018, pp. 4943–4950.

[27] G. F. Young, L. Scardovi, and N. E. Leonard, "Robustness of noisy consensus dynamics with directed communication," in *Proc. Amer. Control Conf.*, Jun. 2010, pp. 6312–6317.

[28] S. Patterson and B. Bamieh, "Network coherence in fractal graphs," in *Proc. 50th IEEE Conf. Decis. Control*, Dec. 2011, pp. 6445–6450.

[29] Z. Zhang and F. Comellas, "Farey graphs as models for complex networks," *Theor. Comput. Sci.*, vol. 412, no. 8, pp. 865–875, Mar. 2011.

[30] Y. Yi, Z. Zhang, Y. Lin, and G. Chen, "Small-world topology can significantly improve the performance of noisy consensus in a complex network," *Comput. J.*, vol. 58, no. 12, pp. 3242–3254, 2015.

[31] Y. Yi, Z. Zhang, L. Shan, and G. Chen, "Robustness of first-and second-order consensus algorithms for a noisy scale-free small-world Koch network," *IEEE Trans. Control Syst. Technol.*, vol. 25, no. 1, pp. 342–350, Jan. 2017.

[32] Y. Yi, Z. Zhang, and S. Patterson, "Scale-free loopy structure is resistant to noise in consensus dynamics in complex networks," *IEEE Trans. Cybern.*, vol. 50, no. 1, pp. 190–200, Sep. 2020.

[33] W. Ren and E. Atkins, "Second-order consensus protocols in multiple vehicle systems with local interactions," in *Proc. AIAA Guid. Navig. Control Conf. Exhibit*, 2005, pp. 15–18.

[34] R. Carli and S. Zampieri, "Network clock synchronization based on the second-order linear consensus algorithm," *IEEE Trans. Autom. Control*, vol. 59, no. 2, pp. 409–422, Feb. 2014.

[35] A.-L. Barabasi and R. Albert, "Emergence of scaling in random networks," *Science*, vol. 286, no. 5439, pp. 509–512, 1999.

[36] D. J. Watts and S. H. Strogatz, "Collective dynamics of 'small-world' networks," *Nature*, vol. 393, no. 6684, pp. 440–442, Jun. 1998.

[37] H. D. Rozenfeld, J. E. Kirk, E. M. Bollt, and D. Ben-Avraham, "Statistics of cycles: How loopy is your network?" *J. Phys. A*, vol. 38, no. 21, p. 4589, 2005.

[38] K. Klemm and P. F. Stadler, "Statistics of cycles in large networks," *Phys. Rev. E Stat. Phys. Plasmas, Fluids, Related Interdiscipl. Top.*, vol. 73, no. 2, 2006, Art. no. 025101.

[39] L. Shan, H. Li, and Z. Zhang, "Domination number and minimum dominating sets in pseudofractal scale-free Web and Sierpinski graph," *Theor. Comput. Sci.*, vol. 677, pp. 12–30, May 2017.

[40] L. Shan, H. Li, and Z. Zhang, "Independence number and the number of maximum independent sets in pseudofractal scale-free Web and Sierpinski gasket," *Theor. Comput. Sci.*, vol. 720, pp. 47–54, Apr. 2018.

[41] P. Xie, Z. Zhang, and F. Comellas, "On the spectrum of the normalized Laplacian of iterated triangulations of graphs," *Appl. Math. Comput.*, vol. 273, pp. 1123–1129, Jan. 2016.

[42] R. Merris, "Laplacian graph eigenvectors," *Linear Algebra Appl.*, vol. 278, nos. 1–3, pp. 221–236, 1998.

[43] D. J. Klein and M. Randić, "Resistance distance," *J. Math. Chem.*, vol. 12, no. 1, pp. 81–95, 1993.

[44] Y. Lipman, R. M. Rustamov, and T. A. Funkhouser, "Biharmonic distance," *ACM Trans. Graph.*, vol. 29, no. 3, p. 27, 2010.

[45] A. Ghosh, S. Boyd, and A. Saberi, "Minimizing effective resistance of a graph," *SIAM Rev.*, vol. 50, no. 1, pp. 37–66, Feb. 2008.

[46] M. Tyloo, T. Coletta, and P. Jacquod, "Robustness of synchrony in complex networks and generalized Kirchhoff indices," *Phys. Rev. Lett.*, vol. 120, no. 8, 2018, Art. no. 084101.

[47] B. Bamieh, M. Jovanovic, P. Mitra, and S. Patterson, 'Effect of topological dimension on rigidity of vehicle formations: Fundamental limitations of local feedback," in *Proc. 47th IEEE Conf. Decision Control*, Dec. 2008, pp. 369–374.

[48] J. Kunegis, "Konect: The Koblenz network collection," in *Proc. 22nd Int. Conf. World Wide Web*, 2013, pp. 1343–1350.

[49] S. N. Dorogovtsev, A. V. Goltsev, and J. F. F. Mendes, "Pseudofractal scale-free Web," *Phys. Rev. E Stat. Phys. Plasmas, Fluids, Related Interdiscipl. Top.*, vol. 65, no. 6, 2002, Art. no. 066122.

[50] Z. Zhang, B. Wu, and Y. Lin, "Counting spanning trees in a small-world Farey graph," *Physica A Stat. Mech. Appl.*, vol. 391, no. 11, pp. 3342–3349, Jun. 2012.

[51] C. Zhan, G. Chen, and L. F. Yeung, "On the distributions of Laplacian eigenvalues versus node degrees in complex networks," *Physica A Stat. Mech. Appl.*, vol. 389, no. 8, pp. 1779–1788, 2010.

[52] H. Li, Q. Lü, and T. Huang, "Convergence analysis of a distributed optimization algorithm with a general unbalanced directed communication network," *IEEE Trans. Netw. Sci. Eng.*, vol. 6, no. 3, pp. 237–248, Jul.–Sep. 2019.

[53] Q. Lü, X. Liao, H. Li, and T. Huang, "A Nesterov-like gradient tracking algorithm for distributed optimization over directed networks," *IEEE Trans. Syst., Man, Cybern., Syst.*, early access, Jan. 8, 2020, doi: 10.1109/TSMC.2019.2960770.

[54] A. Barrat, M. Barthelemy, R. Pastor-Satorras, and A. Vespignani, "The architecture of complex weighted networks," *Proc. Nat. Acad. Sci. USA*, vol. 101, no. 11, pp. 3747–3752, 2004.

[55] Y. Qi, H. Li, and Z. Zhang, "Extended corona product as an exactly tractable model for weighted heterogeneous networks," *Comput. J.*, vol. 61, no. 5, pp. 745–760, 2018.

[56] C. Somarakis, Y. Ghaedsharaf, and N. Motee, "Time-delay origins of fundamental tradeoffs between risk of large fluctuations and network connectivity," *IEEE Trans. Autom. Control*, vol. 64, no. 9, pp. 3571–3586, Sep. 2019.

[57] Q. Lü, X. Liao, T. Xiang, H. Li, and T. Huang, "Privacy masking stochastic subgradient-push algorithm for distributed online optimization," *IEEE Trans. Cybern.*, early access, Mar. 9, 2020, doi: 10.1109/TCYB.2020.2973221.

Wanyue Xu (Graduate Student Member, IEEE) received the B.Eng. degree in computer science and technology from Shangdong University, Weihai, China, in 2019. She is currently pursuing the master's degree with the School of Computer Science, Fudan University, Shanghai, China.

Ms. Xu has published several papers in international journals or conferences, including IEEE TRANSACTIONS ON CYBERNETICS, WWW, WSDM, and ICDM. Her research interests include network science, graph data mining, social network analysis, and random walks.

Bin Wu received the B.S. and M.Sc. degrees in computer science from Fudan University, Shanghai, China, in 2011 and 2014, respectively.

His research interests include complex networks, random walks, and spectral graph theory.

Zuobai Zhang is currently pursuing the B.S. degree with the School of Computer Science, Fudan University, Shanghai, China.

He has published several papers in international journals or conferences, including WSDM, WWW, and IEEE TRANSACTIONS ON CYBERNETICS. His research interests include graph algorithms, social networks, and network science.

Mr. Zhang won a Silver Medal in the National Olympiad in Informatics of China in 2016 and several Gold Medals in ICPC Asia Regional Contests.

Zhongzhi Zhang (Member, IEEE) received the B.Sc. degree in applied mathematics from Anhui University, Hefei, China, in 1997, and the Ph.D. degree in management science and engineering from the Dalian University of Technology, Dalian, China, in 2006.

From 2006 to 2008, he was a Postdoctoral Research Fellow with Fudan University, Shanghai, China, where he is currently a Full Professor with the School of Computer Science. He has published over 140 papers in international journals or conferences. He has over 3000 ISI Web of Science citations with an H-index of 32 according to Clarivate. He was one of the most cited Chinese researchers (Elsevier) in 2019. His current research interests include network science, graph data mining, social network analysis, spectral graph theory, and random walks.

Prof. Zhang was a recipient of the Excellent Doctoral Dissertation Award of Liaoning Province, China, in 2007, the Excellent Post-Doctor Award of Fudan University in 2008, the Shanghai Natural Science Award (third class) in 2013, and the Wilkes Award for the best paper published in *The Computer Journal* in 2019.

Haibin Kan (Member, IEEE) received the Ph.D. degree from Fudan University, Shanghai, China, in 1999.

He became a Faculty with Fudan University. From 2002 to 2006, he was with the Japan Advanced Institute of Science and Technology, Nomi, Japan, as an Assistant Professor. He returned to Fudan University in 2006, where he is currently a Full Professor. His research interests include coding theory, cryptography, and computational complexity.

Guanrong Chen (Life Fellow, IEEE) received the M.Sc. degree in computer science from Sun Yat-sen University, Guangzhou, China, in 1981, and the Ph.D. degree in applied mathematics from Texas A&M University, College Station, TX, USA, in 1987.

He was a Tenured Full Professor with the University of Houston, Houston, TX, USA. He has been a Chair Professor and the Founding Director of the Center for Chaos and Complex Networks, City University of Hong Kong, Hong Kong, since 2000.

Prof. Chen was a recipient of the 2011 Euler Gold Medal from Russia and conferred Honorary Doctorate by Saint Petersburg State University, Russia, in 2011, and by the University of Le Havre, Nomandie, France, in 2014. He is a Highly Cited Researcher in engineering and also in mathematics according to Thomson Reuters. He is a member of Academia Europaea and a Fellow of the World Academy of Sciences.